

Evaluation of Sternheimer Nuclear Quadrupole Shielding Functions and their Application to the Determination of the $^{57}\text{Fe}^m$ Nuclear Quadrupole Moment from X-ray-Determined Charge Densities

ZHENGWEI SU AND PHILIP COPPENS*

Department of Chemistry, Natural Sciences Complex, State University of New York at Buffalo, Buffalo, NY 14260-3000, USA. E-mail: che9990@ubvms.cc.buffalo.edu

(Received 22 February 1996; accepted 8 May 1996)

Abstract

The Sternheimer function $\gamma(r)$ describes the shielding/antishielding of the electric field gradient (EFG) at the nuclear position due to polarization induced in the atomic density by the quadrupolar components of the density distribution. The functions for Fe, Fe^{2+} and Fe^{3+} have been derived by means of Sternheimer's procedure [Sternheimer (1986). *Z. Naturforsch. Teil A*, **41**, 24–36], using a finite-difference method for solving the radial equations for the perturbed wavefunctions and numerical integration for the calculation of $\gamma(r)$. The shielding factors R , due to the contributions from the electron density of the atom at the nucleus of which the EFG is being considered (the 'central contributions'), are derived from the γ functions. Results are given for near-Hartree-Fock atomic and ionic wavefunctions [Clementi & Roetti (1974). *At. Data Nucl. Data Tables*, **14**, 177–478]. Contributions to the shielding from the core and valence electrons are separated. Since the X-ray multipole formalism describes a flexible valence shell but uses a frozen core, only $\gamma_{\infty}^{\text{core}}$ and R^{core} are used in the calculation of Mössbauer splittings from the experimental charge densities. The effect on the shielding of X-ray-determined radial expansion/contraction of the valence shells [Coppens, Guru Row, Leung, Stevens, Becker & Yang (1979). *Acta Cryst.* **A35**, 63–72] is evaluated. The combination of spectroscopic nuclear quadrupole splittings and X-ray charge densities on iron pyrite (FeS_2), sodium nitroprusside $\{[\text{Na}_2\text{Fe}(\text{NO})(\text{CN})_5] \cdot 2\text{H}_2\text{O}\}$ and $[\text{Fe}(\text{TPP})(\text{pyridyl})_2]$ leads to unweighted and weighted average values for $Q(^{57}\text{Fe}^m)$ of 0.12 (3) and $0.11 (2) \times 10^{-28} \text{ m}^2$, respectively, when the core shielding factors are used.

1. Introduction

Accurate X-ray diffraction data can provide the detailed charge distribution in a crystal and therefore electrostatic properties such as molecular moments, the electrostatic potential and its derivatives. Many of these quantities are also accessible by theoretical and other experimental techniques. Among the latter are

Mössbauer and nuclear quadrupole resonance, which are related to the electric field gradient (EFG) tensor elements through the quadrupole moment Q of the excited iron nucleus $^{57}\text{Fe}^m$. Comparison of the X-ray and spectroscopic results provides a mutual check on the procedures used in each method and gives information on the value of the nuclear quadrupole moment. It also establishes the interpretation of the spectroscopically observed hyperfine splittings in terms of the detailed charge-density distribution.

The elements of the traceless electric field gradient tensor, at the position in a crystal defined by \mathbf{r}' , can be written as

$$\nabla \mathbf{E}_{\alpha\beta}^{\text{total}}(\mathbf{r}') = \int \{ [\rho_N(\mathbf{r}) - \rho_e(\mathbf{r})] (3x_\alpha x_\beta - |\mathbf{r} - \mathbf{r}'|^2 \delta_{\alpha\beta}) \times |\mathbf{r} - \mathbf{r}'|^{-5} \} d\mathbf{r}, \quad (1a)$$

where $1 \leq \alpha, \beta \leq 3$, x_α, x_β are the α th and β th components of $\mathbf{r} - \mathbf{r}'$, ρ_N and ρ_e are the nuclear and electronic charge densities, respectively, and δ is the Kronecker delta.

Taking into account the polarization of the electrons induced by both the nuclear and the electronic quadrupolar features of the density distribution (Lauer, Marathe & Trautwein, 1979), the expression for the EFG at the nuclear position becomes (Srivastava, Bhargava, Iyengar & Thosar, 1983; Marathe & Trautwein, 1983)

$$\nabla \mathbf{E}_{\alpha\beta}^{\text{total}}(\mathbf{r}') = \int \{ [\rho_N(\mathbf{r}) - \rho_e(\mathbf{r})] (3x_\alpha x_\beta - |\mathbf{r} - \mathbf{r}'|^2 \delta_{\alpha\beta}) / |\mathbf{r} - \mathbf{r}'|^5 \} \times [1 - \gamma(|\mathbf{r} - \mathbf{r}'|)] d\mathbf{r}, \quad (1b)$$

where $\gamma(r)$ is the Sternheimer shielding/antishielding function (Sternheimer, 1986), which depends on the polarizing distribution at \mathbf{r} and on the wavefunction of the electrons that are polarized. The nuclear charge density ρ_N excludes the charge of the nucleus at which the EFG is being evaluated. A positive/negative value of $\gamma(r)$ corresponds to shielding/antishielding of the nucleus, respectively. $\gamma(r)$ consists of two components,

$$\gamma^{\text{total}}(r) = \gamma^{\text{core}}(r) + \gamma^{\text{valence}}(r), \quad (2)$$

representing the polarization of the core and valence shells, respectively. The polarization of the charge density must be accounted for in the calculation of the EFG at the nuclear position if it is not represented by the basis set used in the theory or the modeling of the experiment.

In the analysis of the X-ray data with the aspherical-atom multipole formalism, further described below (Hansen & Coppens, 1978; Coppens, 1993; Coppens, 1997), the charge density is subdivided into multipolar functions centered on the atomic positions. Following earlier practice (Su & Coppens, 1992), we refer to the *peripheral* contributions as those due to the charge density centered on atoms other than the one at the nucleus of which the EFG is being evaluated and the *central* component as that due to the density on the atom itself.

The effect of the peripheral charge density is often represented by γ_∞ , defined as

$$\gamma_\infty = \lim_{r \rightarrow \infty} \gamma(r), \quad (3)$$

while for the central component a density-weighted average R of $\gamma(r)$ is used. These lead to the simplified expression

$$\begin{aligned} \nabla \mathbf{E}_{\alpha\beta}^{\text{total}}(\mathbf{r}') &= \nabla \mathbf{E}_{\alpha\beta}^{\text{central}}(\mathbf{r}')(1 - R) \\ &+ \nabla \mathbf{E}_{\alpha\beta}^{\text{peripheral}}(\mathbf{r}')(1 - \gamma_\infty), \end{aligned} \quad (4)$$

in which R and γ_∞ are referred to as the Sternheimer nuclear quadrupole shielding/antishielding factors. Expression (4) is a good approximation to (1) if there is little overlap between the central atom and its neighbors.

In the aspherical-atom formalism, the atomic density for each of the atoms is described as (Hansen & Coppens, 1978; Coppens, 1993)

$$\begin{aligned} \rho_{\text{atomic}}(\mathbf{r}) &= P_c \rho_{\text{core}}(r) + \kappa^3 P_v \rho_v(\kappa r) \\ &+ \kappa^3 \sum_{l=0}^{l_{\text{max}}} \sum_{m=0}^l \sum_p P_{lmp} R_{nl}(\kappa' r) d_{lmp}(\theta, \varphi), \end{aligned} \quad (5)$$

where $\rho_{\text{core}}(r)$ and $\rho_v(\kappa r)$ are normalized to one electron, $p = +$ or $-$, κ and κ' are valence-shell expansion/contraction parameters, the density functions d_{lmp} are real spherical harmonics with a normalization appropriate for density functions, P_v and P_{lmp} are electron population parameters and $R_{nl}(\kappa' r)$ are radial functions, which for light atoms are usually expressed in terms of Slater-type functions. For transition-metal atoms, we use the same Hartree-Fock-type radial functions for the spherical valence term and the aspherical deformation functions, as the asphericity is mainly due to preferential occupancy of the valence orbitals, rather than to covalent bonding (Coppens,

1992). This also means that κ and κ' are taken as being equal for transition-metal atoms.

According to (5), the electronic density of an atom in the crystal consists of an unperturbed core-electron density, a valence-shell spherical density modified by a radial expansion/contraction parameter κ (Coppens, Guru Row, Leung, Stevens, Becker & Yang, 1979) and higher-order aspherical components described by an expansion of spherical harmonic functions. The adjustable charge-density parameters κ , κ' , P_v and P_{lmp} are derived by least-squares fitting of the model to the experimental X-ray structure factors. The aspherical d_{lmp} functions include the quadrupolar density components ($l = 2$), which are the contributors to $\nabla \mathbf{E}_{\alpha\beta}^{\text{central}}$.

Since the diffraction data contain virtually no information on the asphericities of the core-electron distribution, the diffraction model contains a frozen core. Thus, core-polarization effects are not accounted for in the model. On the other hand, the valence shell's asphericity is incorporated in the model so its polarization will be reflected in the experimental populations. It is therefore consistent to use $\gamma^{\text{core}}(r)$ and R^{core} , rather than $\gamma^{\text{total}}(r)$ and R^{total} in (2) and (4). As pointed out by Lauer, Marathe & Trautwein (1979), a similar situation exists for molecular-orbital (MO) and band-structure calculations in which the cores are frozen. The shielding factor R^{core} will depend on the expansion/contraction parameter κ of the polarizing valence density.

We introduce in §2 a numerical method for solving the differential equations involved in Sternheimer's procedure for the evaluation of $\gamma(r)$. Results are summarized in §3. In §4, we briefly outline the evaluation of the EFG from X-ray charge density, the results of which for a number of Fe^{II}-containing compounds are presented in §5. §6 discusses the estimation of the nuclear quadrupole moment of the excited state of the Fe atom, ⁵⁷Fe^m.

2. Sternheimer's procedure for the evaluation of $\gamma(r)$

Consider the first-order perturbation equation

$$(H_0 + H_1)(\psi_0 + \psi_1) = (E_0 + E_1)(\psi_0 + \psi_1), \quad (6)$$

where H_0 and ψ_0 are the Hamiltonian and the wavefunction of the unperturbed system, which we approximate as the free atom or ion, and H_1 and ψ_1 the corresponding quantities with the perturbation. As shown by Sternheimer (1966), the shielding factors can be evaluated by considering either the polarizing effect of the nuclear quadrupole moment or that of the charge distribution external to the nucleus. A nuclear quadrupole moment Q induces a quadrupole moment in a polarizable charge distribution, which in the expression for the quadrupole splitting is represented by the perturbation operator

$$H_1 = -Q(3 \cos^2 \theta - 1)/4r^3, \quad (7)$$

where atomic units have been used (Sternheimer, 1950). In (7), the quantity in brackets is twice the Legendre polynomial $P_2(\cos \theta)$, r is the length of a vector from the nucleus to a point at which the wavefunction is defined and θ is the angle between that vector and the axis of the nuclear quadrupole moment.

Sternheimer has shown that (6) and (7) lead, for a shell with quantum numbers n and l for ψ_0 and n and l' for ψ_1 , to the radial expression (Sternheimer, 1986)

$$\left(\frac{d^2}{dr^2} + \frac{l'(l'+1) - l(l+1)}{r^2} + \frac{1}{u_{0,nl}} \frac{d^2 u_{0,nl}(r)}{dr^2} \right) u_{1,nl \rightarrow l'}(r) = u_{0,nl}(1/r^3 - \langle r^{-3} \rangle_{nl} \delta_{ll'}), \quad (8)$$

where $u_{0,nl}(r)$ is r times the radial part of the n, l component of ψ_0 , $u_{1,nl \rightarrow l'}(r)$ is r times the radial part of the corresponding component of ψ_1 . $l' = l, l+2$ for $0 \leq l < 2$ and $l' = l, l+2, l-2$ for $l \geq 2$.

For the radial excitations ($l = l'$), the excited-state functions u_1 must be orthogonalized to the ground-state function

$$u'_{1,nl \rightarrow l}(r) = u_{1,nl \rightarrow l}(r) - a u_{0,nl}(r), \quad (9)$$

where

$$a = \int_0^\infty u_{1,nl \rightarrow l}(r) u_{0,nl}(r) dr. \quad (10)$$

For the angular excitations ($l \neq l'$), orthogonalization is inherent in the change in quantum number. Thus,

$$u'_{1,nl \rightarrow l'}(r) = u_{1,nl \rightarrow l'}(r) \text{ with } l' = l \pm 2. \quad (11)$$

$\gamma_{nlm}(r)$, the electrostatic contribution from one electron with quantum numbers nlm , is given by (Sternheimer, 1967)

$$\gamma_{nlm}(r) = \sum_{l'} c_{ll'm} \left\{ \int_0^r u_{0,nl}(r') u'_{1,nl \rightarrow l'}(r') r'^2 dr' + r^5 \int_r^\infty [u_{0,nl}(r') u'_{1,nl \rightarrow l'}(r') / r'^3] dr' \right\}, \quad (12a)$$

where

$$c_{ll'm} = 4 \left(I_{ll'}^{(2)m} \right)^2 \quad (12b)$$

and

$$I_{ll'}^{(2)m} = \int_0^\pi P_2(\cos \theta) \Theta_{lm}(\theta) \Theta_{l'm}(\theta) \sin \theta d\theta. \quad (12c)$$

$\Theta_{lm}(\theta)$ are the normalized associated Legendre functions defined by

$$\Theta_{lm}(\theta) = \{ [(2l+1)/2](l-m)!/(l+m)! \}^{1/2} P_l^m \cos(\theta) \quad (12d)$$

and

$$P_2(\cos \theta) = (3 \cos^2 \theta - 1)/2. \quad (12e)$$

Table 1. Values of the coefficient $C(l \rightarrow l')$ [$= C(l' \rightarrow l)$] in (13) for $\gamma(r)$

l	l'	Excitation	$C(l \rightarrow l')$
0	2	$s \rightarrow d$	8/5
1	1	$p \rightarrow p$	48/25
1	3	$p \rightarrow f$	72/25
2	2	$d \rightarrow d$	16/7
2	4	$d \rightarrow g$	144/35
3	3	$f \rightarrow f$	224/75
3	5	$f \rightarrow h$	16/3

The total electrostatic contribution to $\gamma(r)$ due to a filled nl shell (with $4l+2$ electrons) is obtained as a sum over the individual electron contributions

$$\gamma(r) = \sum_{l'} C(l \rightarrow l') \left\{ \int_0^r u_{0,nl}(r') u'_{1,nl \rightarrow l'}(r') r'^2 dr' + r^5 \int_r^\infty [u_{0,nl}(r') u'_{1,nl \rightarrow l'}(r') / r'^3] dr' \right\}. \quad (13)$$

Comparison of (12a) and (13), taking into account the spin degeneracy, gives for the coefficients C

$$C(l \rightarrow l') = 2 \sum_{m=-l}^l c_{ll'm}. \quad (14)$$

Some values of $C(l \rightarrow l')$ are given in Table 1. $C(l \rightarrow l')$ is independent of n and $C(l \rightarrow l') = C(l' \rightarrow l)$, as is evident from the preceding equations.

The shielding factor R consists of a contribution R_D , due to the electrostatic interaction, and a contribution R_E , due to exchange interactions between electrons with the same spin quantum number, or

$$R = R_D + R_E. \quad (15)$$

For polarization by the EFG of the electrons with quantum numbers n_v, l_v ,

$$R_{D,nlm} = \langle \gamma(r) r^{-3} \rangle_{\text{valence}} / \langle r^{-3} \rangle_{\text{valence}} = (1 / \langle r^{-3} \rangle_{n_v, l_v}) \int_0^\infty \gamma_{nlm}(r) w_{n_v, l_v}^2(r) r^{-3} dr, \quad (16)$$

where w_{n_v, l_v} is r times the radial part of the wavefunction of the valence electrons contributing to the EFG at the nuclear position, with quantum numbers n_v and l_v ; r^{-3} is the interaction operator from the perturbation Hamiltonian H_1 , defined in (7).

The contribution to R_E due to the exchange between two electrons with different spin is 0. For parallel spins, the contribution is non-zero and given by

$$R_{E,nl \rightarrow l'm} = \sum_L (b_{ll'l_v L} / \langle r^{-3} \rangle_{n_v, l_v}) \int_0^\infty u_{0,nl}(r) w_{n_v, l_v}(r) g_L(r) dr \quad (17a)$$

with

$$g_L(r) = (1/r^{L+1}) \int_0^r u'_{1,nl \rightarrow l'}(r') w_{n,l_v}(r') r'^L dr' + r^L \int_r^\infty u'_{1,nl \rightarrow l'}(r') w_{n,l_v}(r') r'^{-L-1} dr' \quad (17b)$$

and

$$b_{ll',L} = 2c^{(2)}(lm; l'm') c^{(L)}(lm; l_v m_v) c^{(L)}(l'm; l_v m_v) \times [c^{(2)}(l_v m_v; l_v m_v)]^{-1} \quad (17c)$$

with (Sternheimer, 1967)

$$c^{(L)}(lm; l'm') = [2/(2L+1)]^{1/2} \times \int_0^\pi \Theta_L^{m-m'}(\theta) \Theta_l^m(\theta) \Theta_{l'}^{m'}(\theta) \sin \theta d\theta. \quad (17d)$$

The contribution to R_E due to a filled nl shell is (Sternheimer, 1967)

$$\sum_L [B(l \rightarrow l'; l_v; L) / \langle r^{-3} \rangle_{n,l_v}] \int_0^\infty u_{0,nl}(r) w_{n,l_v} g_L(r) dr. \quad (18)$$

The coefficients $B(l \rightarrow l'; l_v; L)$ are summarized in Table 2.

2.1. The numerical method

We use the finite-difference method (Burden & Faires, 1989; Press, Flannery, Teukolsky & Vetterling, 1986) in solving the differential equation (8). Analysis of the limits of both sides of (8) as $r \rightarrow 0$ shows that the boundary conditions can be chosen as

for $l \neq 0$:

$$u_1(r_0) = 0, \quad u_1(r_0 + r_1) = 0; \quad (19a)$$

for $l = 0$:

$$u_1(r_0) = \frac{1}{\delta} \lim_{r \rightarrow r_0} [u_0(r)/r], \quad u_1(r_0 + r_1) = 0. \quad (19b)$$

r_0 is a very small positive value, typically taken as 1.0×10^{-6} a.u.; r_1 is chosen to be sufficiently far away from the nucleus for the wavefunction to be essentially equal to zero. We have used $r_1 = 10.0$ a.u. and a step size of 2.0×10^{-3} a.u. to obtain the numerical values of u_1 , the excited-state radial functions at each of the points. The integrations in (10), (12a), (13), (16), (17a) and (17b) were performed using the composite Simpson formula as described in Burden & Faires (1989).

Test calculations using different values of r_0 , r_1 and step size show the resulting values of $\gamma(r)$ and R to be accurate to 1% or better.

Table 2. Values of $B(l \rightarrow l'; l_v; L [= B(l' \rightarrow l; l_v; L)])$ in (18) for R_E

This table is an extension to the table given by Sternheimer (1967).

$l \rightarrow l'$	l_v	L	$B(nl \rightarrow l'; l_v; L)$	
0	2	1	1	4/3
1	1	1	0	4
1	1	1	2	4/25
1	3	1	2	36/25
2	2	1	1	4/3
2	2	1	3	12/49
2	4	1	3	72/49
3	3	1	2	24/25
3	3	1	4	8/27
3	5	1	4	40/27
0	2	2	2	4/5
1	1	2	1	28/25
1	1	2	3	36/175
1	3	2	1	12/25
1	3	2	3	36/175
2	2	2	0	4
2	2	2	2	-12/49
2	2	2	4	16/49
2	4	2	2	144/245
2	4	2	4	40/49
3	3	2	1	48/25
3	3	2	3	-88/225
3	3	2	5	40/99
3	5	2	3	40/63
3	5	2	5	80/99
0	2	3	3	4/7
1	1	3	2	108/175
1	1	3	4	4/21
1	3	3	2	72/175
1	3	3	4	4/7
2	2	3	1	72/49
2	2	3	3	-44/147
2	2	3	5	500/1617
2	4	3	1	12/49
2	4	3	3	24/49
2	4	3	5	300/539
3	3	3	0	4
3	3	3	2	76/225
3	3	3	4	-4/11
3	5	3	2	20/63
3	5	3	4	40/77
3	5	3	6	700/1287

3. $\gamma(r)$ and R for the Fe atom in various ionization states

3.1. Fe^{2+}

We use as the unperturbed wavefunctions the near-Hartree-Fock wavefunctions for the 5D ground state of Fe^{2+} given by Clementi & Roetti (1974). Tables 3 and 4 give the results for γ_∞ and R , while numerical values for $\gamma(r)$ are listed in Table S1.* The functions $\gamma^{core}(r)$ and $\gamma^{core+valence}(r)$ are shown in Fig. 1.

*The supplementary material giving $\gamma(r)$ for Fe^{2+} from core and valence electrons has been deposited with the IUCr (Reference: BK0033). Copies may be obtained through The Managing Editor, International Union of Crystallography, 5 Abbey Square, Chester CH1 2HU, England.

Table 3. Sternheimer nuclear quadrupole factor R and its direct (R_D) and exchange (R_E) contributions for free Fe^{2+}

Excitations	R_D	R_E	$R = R_D + R_E$
$1s \rightarrow d$	0.0257	-0.0008	0.0250
$2s \rightarrow d$	0.0433	-0.0117	0.0316
$3s \rightarrow d$	0.0189	-0.0071	0.0118
$2p \rightarrow f$	0.0640	-0.0135	0.0506
$3p \rightarrow f$	0.0328	-0.0121	0.0207
$2p \rightarrow p$	-0.3178	0.2437	-0.0742
$3p \rightarrow p$	0.1814	-0.1664	0.0150
$3d \rightarrow s$	-0.0096	0.0000	-0.0096
$3d \rightarrow g$	0.0178	0.0000	0.0178
$3d \rightarrow d$	0.0361	0.0000	0.0361

Table 4. Sternheimer nuclear quadrupole factors R and γ_∞ for Fe , Fe^{2+} and Fe^{3+} , all with $\kappa = 1.0$

	R	R	γ_∞	γ_∞
	This work	Literature	This work	Literature
Fe , $\langle r^{-3} \rangle_{3d} = 4.979$ a.u.				
Total core	0.0730		-8.933	-8.26 ^c
Total valence*	0.0521		-1.294	
Total core + valence	0.1251		-10.227	
Fe^{2+} , $\langle r^{-3} \rangle_{3d} = 5.086$ a.u.				
Total core	0.0704	0.0770 ^a	-8.681	-8.690 ^a
		0.0754 ^b		-8.07 ^c
Total valence	0.0442	0.0536 ^a	-2.354	-2.282 ^a
		0.0508 ^b		
Total core + valence	0.1146	0.1206 ^a	-11.035	-10.972 ^a
		0.1262 ^b		
Fe^{3+} , $\langle r^{-3} \rangle_{3d} = 5.728$ a.u.				
Total core			-7.974	-7.43 ^c
Total valence			-1.453	
Total core + valence			-9.427	-9.14 ^d
				-9.64 ^c

References: (a) Sternheimer (1967); (b) Lauer, Marathe & Trautwein (1979); (c) Lauer, Marathe & Trautwein (1980); (d) Sternheimer (1963); (e) Sen & Narasimhan (1976). *Including the two 4s electrons.

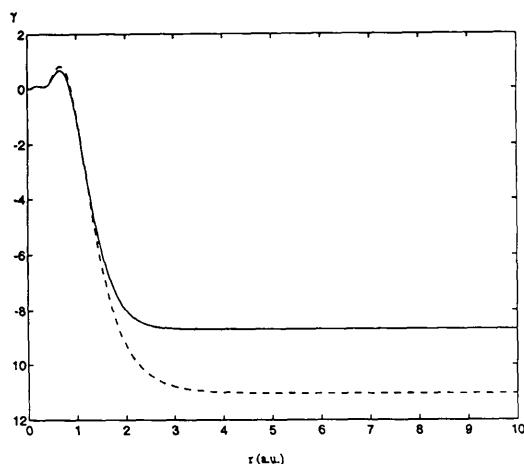


Fig. 1. Sternheimer function $\gamma(r)$ for Fe^{2+} . Solid line: contribution due to polarization of the core electrons, $\gamma^{\text{core}}(r)$; dashed line: contribution due to polarization of the core and valence electrons, $\gamma^{\text{total}}(r)$.

As pointed out by Sternheimer (1972), the contributions to R_D and R_E from the excitation of the valence $3d$ shell can be treated as the interaction of one $3d$ electron with the remaining five $3d$ electrons with opposite spins. Thus, there is no contribution to R_E from $3d \rightarrow s$, $3d \rightarrow d$ and $3d \rightarrow g$ excitations, and the contributions to R_D from these five valence electrons is half that of a filled $3d$ shell.

A second calculation, not separately reported here, using the low-spin 1F excited-state wavefunction for the Fe^{2+} ion, leads to shielding factors very similar to those for the 5D ground state. This result supports the application of the free-ion core-shielding factors to iron in molecular complexes.

3.1.1. *Dependency of R and γ_∞ on κ .* For non-unity values of κ in (5), the radial part of the electron-density function, and thus the radial part of the wavefunction, is modified relative to the free-atom functions. If the basis-set functions are Slater type, the radial part of the wavefunction with quantum numbers n , l for the unperturbed atom,

$$(2n!)^{-0.5} (2\zeta)^{(n+0.5)} r^{n-1} \exp(-\zeta r), \quad (20a)$$

becomes

$$(2n!)^{-0.5} (2\kappa\zeta)^{n+0.5} r^{n-1} \exp(-\kappa\zeta r). \quad (20b)$$

Because of the flexibility of the valence shell in the multipole model, R^{valence} and $\gamma^{\text{valence}}(r)$ do not enter the equations relevant to the X-ray case. The core distribution is fixed at $\kappa_{\text{core}} = 1$ but R^{core} , which represents the polarization of the core electrons by the valence distribution on the central atom, is a function of the κ values of the valence shell.

Values of R_D^{core} , R_E^{core} and their sum, R^{core} , for Fe^{2+} for a number of κ values in the range 0.8–1.2 are summarized in Table 5. The values for Fe^{2+} in this range are well fitted (to about 1 in 10^4) by the polynomial

$$R^{\text{core}}(Fe^{2+}, \kappa) = 1.0686 - 2.4955\kappa + 2.06100\kappa^2 - 0.56369\kappa^3. \quad (21)$$

Expression (21) is illustrated in Fig. 2.

3.2. Fe^{3+} and Fe

The calculation for Fe is the same as that for Fe^{2+} except for the contribution of the $4s^2$ electrons to $\gamma(r)$ and R . R is not defined for a free Fe^{3+} in its ground (6S) state because of the absence of asphericity of the valence shell.

The results are included in Table 4, while γ^{core} for the three valence states is plotted in Fig. 3. Examination of the figure shows that

$$|\gamma_\infty^{\text{core}}(Fe)| > |\gamma_\infty^{\text{core}}(Fe^{2+})| > |\gamma_\infty^{\text{core}}(Fe^{3+})|,$$

Table 5. R_D^{core} , R_E^{core} and R^{core} for Fe^{2+} with different κ values

κ	0.8	0.85	0.9	0.925	0.95	0.975	1.0
$\langle r^{-3} \rangle_{3d,\kappa}^*$ (a.u.)	2.604	3.123	3.708	4.025	4.360	4.714	5.086
R_D^{core}	-0.130	-0.0654	-0.0164	0.0034	0.0206	0.0355	0.0483
R_E^{core}	0.233	0.1557	0.0975	0.0741	0.0540	0.0368	0.0221
R^{core}	0.103	0.0903	0.0811	0.0775	0.0746	0.0723	0.0704
κ	1.025	1.05	1.075	1.1	1.15	1.20	
$\langle r^{-3} \rangle_{3d,\kappa}^*$ (a.u.)	5.477	5.887	6.318	6.769	7.735	8.788	
R_D^{core}	0.0594	0.0689	0.0770	0.0840	0.0948	0.1024	
R_E^{core}	0.0096	-0.0009	-0.0096	-0.0169	-0.0277	-0.0346	
R^{core}	0.0690	0.0680	0.0674	0.0671	0.0671	0.0678	

* $\langle r^{-3} \rangle_{3d,\kappa} = \kappa^3 \langle r^{-3} \rangle_{3d} = 5.086\kappa^3$ (a.u.).

indicating that the polarizability of the core density is reduced by an increase in oxidation number. This is as expected from the increase in binding energy of the electrons with oxidation state.

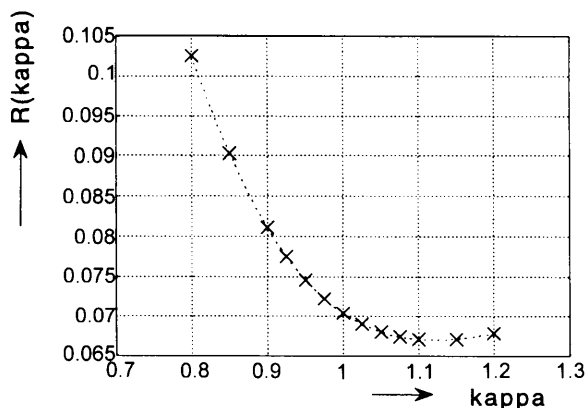


Fig. 2. Dependence of the shielding factor $R^{\text{core}}(\text{Fe}^{2+})$ on the valence-shell expansion/contraction parameter κ .

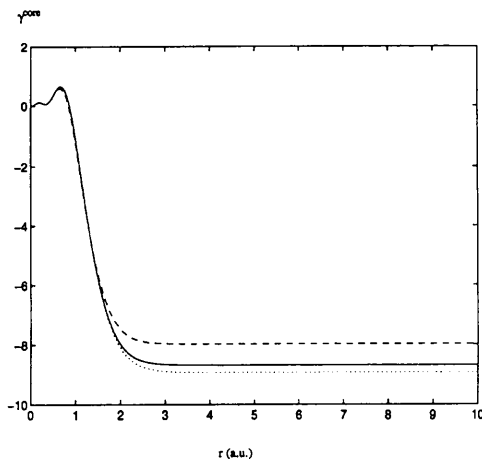


Fig. 3. Sternheimer functions $\gamma^{\text{core}}(r)$ for Fe (dots), Fe^{2+} (solid line) and Fe^{3+} (dashed line). Curves are for $\kappa = 1$.

For all species, γ_∞ is dominated by the antishielding radial excitations $3p \rightarrow p$ and $2p \rightarrow p$. The angular excitations are shielding except for $3d \rightarrow s$.

The κ dependence of $R^{\text{core}}(\text{Fe})$ is well fitted by a polynomial similar to (21):

$$R^{\text{core}}(\text{Fe}, \kappa) = 1.1061 - 2.5832\kappa + 2.1352\kappa^2 - 0.58519\kappa^3. \quad (22)$$

4. Calculation of the EFG from the multipole description of the charge density

The method for calculating the electric field gradient from the model density in (5) is described in the literature (Epstein & Swanton, 1982; Su & Coppens, 1992; Su, 1993a). Only the quadrupolar density components [$l = 2$ in (5)] contribute to the EFG component due to the parent atom, $\nabla E_{\alpha\beta}^{\text{central}}$. The central contributions are given by

$$\begin{aligned} \nabla E_{xx} &= + (3/5)(\pi P_{22+} - 3^{1/2} P_{20}) \langle r^{-3} \rangle \\ \nabla E_{yy} &= - (3/5)(\pi P_{22+} + 3^{1/2} P_{20}) \langle r^{-3} \rangle \\ \nabla E_{zz} &= + (6/5)(3^{1/2} P_{20}) \langle r^{-3} \rangle \\ \nabla E_{xy} &= + (3/5)(\pi P_{22-}) \langle r^{-3} \rangle \\ \nabla E_{xz} &= + (3/5)(\pi P_{21+}) \langle r^{-3} \rangle \\ \nabla E_{yz} &= + (3/5)(\pi P_{21-}) \langle r^{-3} \rangle, \end{aligned} \quad (23)$$

where $\langle r^{-3} \rangle$ is the expectation value for the density function used for the $l = 2$ term in (5). For Fe^{2+} , $\langle r^{-3} \rangle$ is listed in Table 5.

The remainder of the crystal contributes to the quantities $\nabla E_{\alpha\beta}^{\text{peripheral}}$. A density component centered at \mathbf{R}_M , defined by

$$\mathbf{r}_M^N \exp(-\zeta r_M) d_{l_1 m_1 p_1}(\theta_{r_M}, \varphi_{r_M}) \quad (24)$$

[where $\mathbf{r}_M = \mathbf{r} - \mathbf{R}_M$, $r_M = |\mathbf{r}_M|$ and $d_{l_1 m_1 p_1}(\theta, \varphi)$ is a real spherical-harmonic function], contributes to $\nabla E_{\alpha\beta}^{\text{peripheral}}(\mathbf{R}_i)$ an amount that contains a factor

$$A_{N, l_1, l_2, 2}(\zeta, |\mathbf{R}_M - \mathbf{R}_i|) = \int_0^\infty \left[\int_0^\infty r^{N+2} \exp(-\zeta r) j_{l_1}(Sr) dr \right] \times j_{l_2}(S|\mathbf{R}_M - \mathbf{R}_i|) S^2 dS, \quad (25)$$

where $l_2 = |l_1 + 2|, \dots, |l_1 - 2|$. j_l are spherical Bessel functions of order l , and S is the dummy variable of integration.

The expressions for $A_{N, l_1, l_2, 2}$ for $N \leq 7$ and $l_1 \leq N$ are listed in the literature (Su & Coppens, 1994) and are incorporated in the program *MOLPROP93* (Su, 1993b) used for the EFG calculations.

5. Application of the expressions

In the present study, the expressions are applied to data sets on pyrite (FeS_2) (Stevens, DeLucia &

Table 6. Central and peripheral contributions to the EFG (a.u.) at the iron nuclear position in the three compounds studied

	Central	Peripheral
FeS ₂	$\begin{pmatrix} -0.27(21) & 0 & 0 \\ 0 & -0.27(21) & 0 \\ 0 & 0 & 0.54(42) \end{pmatrix}$	$\begin{pmatrix} 0.004(11) & 0 & 0 \\ 0 & 0.004(11) & 0 \\ 0 & 0 & -0.008(22) \end{pmatrix}$
[Na ₂ Fe(NO)(CN) ₅].2H ₂ O	$\begin{pmatrix} 0.95(2) & 0 & 0 \\ 0 & 0.95(2) & 0 \\ 0 & 0 & -1.9(4) \end{pmatrix}$	$\begin{pmatrix} 0.014(1) & -0.002(1) & 0.003(1) \\ -0.002(1) & 0.014(1) & -0.003(1) \\ 0.003(1) & -0.003(1) & -0.028(2) \end{pmatrix}$
[Fe(TPP)(py) ₂]	$\begin{pmatrix} -0.60(15) & 0 & 0 \\ 0 & -0.60(15) & 0 \\ 0 & 0 & 1.2(3) \end{pmatrix}$	$\begin{pmatrix} 0.016(5) & -0.001(4) & 0.001(4) \\ -0.001(4) & 0.015(5) & -0.002(4) \\ 0.001(4) & -0.002(4) & -0.031(10) \end{pmatrix}$

Table 7. Comparison of X-ray and Mössbauer quadrupole splittings for Fe^{II} complexes, using $Q = 0.15 \times 10^{-28} \text{ m}^2$ to obtain the X-ray values

	Without Sternheimer correction			With Sternheimer correction			
	∇E_{zz} (a.u.)	η	$\Delta E_{\text{QS}}^{\text{X-ray}}$ (mm s ⁻¹)	∇E_{zz} (a.u.)	η	$\Delta E_{\text{QS}}^{\text{X-ray}}$ (mm s ⁻¹)	$\Delta E_{\text{QS}}^{\text{spec}}$ (mm s ⁻¹)
FeS ₂ *	0.54 (42)	-	-0.82 (64)	0.51 (39)	-	-0.76 (59)	±0.634 (6)
[Fe(NO)(CN) ₅] ²⁻	-1.9 (4)	0.002 (1)	+2.9 (6)	-2.0 (4)	0.019 (4)	+3.0 (6)	±1.717 (4)
[Fe(TPP)(py) ₂]	1.17 (30)	0.017 (4)	-1.8 (5)	0.78 (27)	0.02 (1)	-1.2 (4)	±1.15 (2)

* References to X-ray charge density: FeS₂: Stevens, DeLucia & Coppens (1980), new refinement of data. [Na₂Fe(NO)(CN)₅].2H₂O: Bolotovskiy, Su, Darovskiy & Coppens (1996), 100 K imaging-plate data set collected with synchrotron radiation. [Fe(TPP)(py)₂]: Li (1989), Li, Coppens & Landrum (1988).

Coppens, 1980), sodium nitroprusside {Na₂[Fe(NO)(CN)₅].2H₂O} (Bolotovskiy, Su, Darovskiy & Coppens, 1996) and [Fe(TPP)(pyridyl)₂] (Li, 1989; Li, Coppens & Landrum, 1988) (TPP=tetraphenylporphyrin). In all cases considered here, we have found the substitution of γ_{∞} for $\gamma(r)$ in the peripheral contribution adequate within 1%. This is the case even for sodium nitroprusside, which has the shortest metal–ligand distances of the compounds considered [Fe–N=1.668 (1) Å].

In Table 6, the central and peripheral contributions to the EFG before the Sternheimer correction are listed. The Fe atom in FeS₂ is located on a threefold axis, so all contributions are by necessity diagonal. Because of the local symmetry, this is also the case for the central contributions of the other two complexes. The peripheral contributions are quite small but are enhanced by the antishielding. Table 7 lists the principal elements ∇E_{zz} and the asymmetry parameters η , defined as

$$\eta = (\nabla E_{xx} - \nabla E_{yy}) / \nabla E_{zz}, \quad (26)$$

in which ∇E_{zz} , ∇E_{yy} , ∇E_{xx} are the principal elements of the EFG tensor in order of decreasing absolute value.

The quadrupole splitting ΔE_{QS} for ⁵⁷Fe is given by

$$\Delta E_{\text{QS}} = \frac{1}{2} e V_{zz} Q(^{57}\text{Fe}^m) (1 + \eta^2/3)^{1/2}, \quad (27a)$$

where $V_{zz} = -\nabla E_{zz}$ and $Q(^{57}\text{Fe}^m)$ is the nuclear quadrupole moment for the nucleus in the excited state, which has a spin of 3/2. We initially use $Q(^{57}\text{Fe}^m) = 0.15 \times 10^{-28} \text{ m}^2$ (Lauer, Marathe & Trautwein, 1979; Ray & Das, 1977) but in the next section discuss the implication of the comparison of the spectroscopic and X-ray-derived values of ΔE_{QS} .

After conversion to the Doppler-speed unit (mm s⁻¹), we obtain

$$\Delta E_{\text{QS}}^{\text{X-ray}} = -1.52 \nabla E_{zz} (1 + \eta^2/3)^{1/2}, \quad (27b)$$

where ∇E_{zz} is expressed in a.u. Table 7 lists the values of $\Delta E_{\text{QS}}^{\text{X-ray}}$ calculated from the X-ray data with and without inclusion of the shielding/antishielding effect of the core electrons.

6. Estimation of $Q(^{57}\text{Fe}^m)$ based on the X-ray results

The nuclear quadrupole moment $Q(^{57}\text{Fe}^m)$ cannot be directly measured owing to the short lifetime of the excited nuclear state. Values ranging from -0.19×10^{-28} to $+0.44 \times 10^{-28} \text{ m}^2$ have been reported in the literature (Rusakov & Khramov, 1992). They are based either on models of the nuclear charge distribution or on observed nuclear quadrupole splittings

Table 8. Values of $Q(^{57}\text{Fe}^m)$ calculated according to expression (28) in 10^{-28} m^2

	No Sternheimer correction	With Sternheimer correction
FeS_2	0.12 (9)	0.13 (10)
$[\text{Fe}(\text{TPP})(\text{py})_2]$	0.10 (3)	0.14 (3)
$[\text{Fe}(\text{NO})(\text{CN})_5]^{2-}$	0.09 (2)	0.09 (2)
Straight average	0.10 (2)	0.12 (3)
Weighted average	0.09 (2)	0.11 (2)

combined with electronic structure calculations of various complexity.

As pointed out by Tsirel'son, Strel'tsov, Makarov & Ozerov (1987), an estimate of $Q(^{57}\text{Fe}^m)$ can be derived by comparing spectroscopic and X-ray-derived quadrupole splittings. As the values of $\Delta E_{\text{QS}}^{\text{X-ray}}$ are linearly dependent on $Q(^{57}\text{Fe}^m)$, a best estimate of $Q(^{57}\text{Fe}^m)$ based on X-ray data derived with an initial value of $Q(^{57}\text{Fe}^m) = 0.15 \times 10^{-28} \text{ m}^2$ can be obtained from

$$Q(^{57}\text{Fe}^m) \simeq 0.15 \times 10^{-28} \text{ m}^2 \times (\Delta E_{\text{QS}}^{\text{spec}} / \Delta E_{\text{QS}}^{\text{X-ray}}), \quad (28)$$

assuming $\Delta E_{\text{QS}}^{\text{spec}}$ to have the same sign as $\Delta E_{\text{QS}}^{\text{X-ray}}$. The results are summarized in Table 8.

When the shielding/antishielding effects of the core are not taken into account, the data in Table 7 lead to an unweighted average of $Q(^{57}\text{Fe}^m) = 0.10(2) \times 10^{-28} \text{ m}^2$ and a weighted average of $0.09(2) \times 10^{-28} \text{ m}^2$ (Table 8). The corresponding numbers with shielding are $0.12(3) \times 10^{-28}$ and $0.11(2) \times 10^{-28} \text{ m}^2$. The latter results, which take the polarization of the core into account, are within $1-2\sigma$ of the value of $0.14(2) \times 10^{-28} \text{ m}^2$ reported by Tsirel'son *et al.* (1987), based on earlier X-ray data sets on sodium nitroprusside and Fe_2O_3 , but omitting the shielding and antishielding effects due to the polarization of the core-electron density.

Our results may be compared with the theoretical nuclear value of $0.177 \times 10^{-28} \text{ m}^2$ obtained by Bolotin, Stuchbery, Amos & Morrison (1978) and the much smaller value of $0.082 \times 10^{-28} \text{ m}^2$ of Duff, Mishra & Das (1981), which is based on spectroscopic observations on FeCl_2 and FeBr_2 in a rare-gas matrix and theoretical electron-density distributions for the isolated molecules. The latter have been criticized by Ellis, Guenzburger & Jansen (1983) and by Dufek, Blaha & Schwarz (1995). The latter authors, from comparison of spectroscopic values with EFG's from linearized augmented plane-wave (LAPW) theoretical densities on a series of solids, obtain the value of $0.16 \pm 5\% \times 10^{-28} \text{ m}^2$.

7. Concluding remarks

The separation of the nuclear shielding factors R into core and valence contributions allows their use in the

calculation of the EFG from charge densities described by the multipole formalism. The quantitative comparison between X-ray and spectroscopic results requires accurate knowledge of the nuclear quadrupole moment of the excited state of $^{57}\text{Fe}^m$. But the two sets of results are consistent and can be used to derive a new value for $^{57}\text{Fe}^m$. Our value is somewhat lower than those from the most recent theoretical calculations, possibly as a result of unrecognized errors in the sodium nitroprusside experimental density, which led to the lowest estimate based on the X-ray data (Table 8). Nevertheless, the combined experimental and theoretical evidence clearly points to a value in the range of $0.12-0.17 \times 10^{-28} \text{ m}^2$. As more X-ray-determined charge densities on iron-containing solids are included in the analysis, the X-ray value will become more precise.

Finally, we note that the experimental and theoretical densities provide an interpretation of the observed spectroscopic quadrupole splittings in terms of the detailed charge distribution in the solid.

Support of this work by the National Science Foundation (CHE9317770) is gratefully acknowledged.

References

- Bolotin, H. H., Stuchbery, A. E., Amos, K. & Morrison, I. (1978). *Nucl. Phys.* **A311**, 75-92.
- Bolotovskiy, R., Su, Z., Darovsky, A. & Coppens, P. (1996). In preparation.
- Burden, R. L. & Faires, J. D. (1989). *Numerical Analysis*, 4th ed. Boston: PSW-KENT Publishing Company.
- Clementi, E. & Roetti, C. (1974). *At. Data Nucl. Data Tables*, **14**, 177-478.
- Coppens, P. (1992). *Ann. Rev. Phys. Chem.* **43**, 663-692.
- Coppens, P. (1993). *International Tables for X-ray Crystallography*, Vol. B: *Reciprocal Space*, edited by U. Shmueli, ch. 1.2, pp. 10-22. Dordrecht: Kluwer Academic Publishers.
- Coppens, P. (1997). *X-ray Charge Densities and Chemical Bonding*. Oxford University Press. In the press.
- Coppens, P., Guru Row, T. N., Leung, P., Stevens, E. D., Becker, P. J. & Yang, Y. W. (1979). *Acta Cryst.* **A35**, 63-72.
- Dufek, P., Blaha, P. & Schwarz, K. (1995). *Phys. Rev. Lett.* **75**, 3545-3548.
- Duff, K. J., Mishra, K. C. & Das, T. P. (1981). *Phys. Rev. Lett.* **25**, 1611-1614.
- Ellis, D. E., Guenzburger, D. & Jansen, H. B. (1983). *Phys. Rev. B*, **28**, 3697-3705.
- Epstein, J. & Swanton, D. J. (1982). *J. Chem. Phys.* **77**(2), 1048-1060.
- Hansen, N. K. & Coppens, P. (1978). *Acta Cryst.* **A34**, 909-921.
- Lauer, S., Marathe, V. R. & Trautwein, A. (1979). *Phys. Rev. A*, **19**, 1852-1861.
- Lauer, S., Marathe, V. R. & Trautwein, A. (1980). *Phys. Rev. A*, **22**, 2355-2361.

- Li, N. (1989). PhD thesis, State University of New York at Buffalo, USA.
- Li, N., Coppens, P. & Landrum, J. (1988). *Inorg. Chem.* **27**, 482-488.
- Marathe, V. R. & Trautwein, A. (1983). *Advances in Mössbauer Spectroscopy: Application to Physics, Chemistry and Biology*, edited by B. V. Thosar, P. K. Iyengar, J. K. Srivastava & S. C. Bhargava, pp. 399-454. Oxford: Elsevier.
- Press, W. H., Flannery, B. P., Teukolsky, S. A. & Vetterling, W. T. (1986). *Numerical Recipes, the Art of Scientific Computing*. Cambridge University Press.
- Ray, S. N. & Das, T. P. (1977). *Phys. Rev. B*, **16**, 4794-4804.
- Rusakov, V. S. & Khramov, D. A. (1992). *Bull. Russ. Acad. Sci. Phys.* **56**(7), 1118-1120.
- Sen, K. D. & Narasimhan, P. T. (1976). *Phys. Rev. A*, **14**, 539-542.
- Srivastava, J. K., Bhargava, S. C., Iyengar, P. K. & Thosar, B. V. (1983). *Advances in Mössbauer Spectroscopy: Application to Physics, Chemistry and Biology*, edited by B. V. Thosar, P. K. Iyengar, J. K. Srivastava & S. C. Bhargava, pp. 1-121. Oxford: Elsevier.
- Sternheimer, R. M. (1950). *Phys. Rev.* **80**, 102-103.
- Sternheimer, R. M. (1963). *Phys. Rev.* **130**, 1423-1425.
- Sternheimer, R. M. (1966). *Phys. Rev.* **146**, 140-149.
- Sternheimer, R. M. (1967). *Phys. Rev.* **164**, 10-20.
- Sternheimer, R. M. (1972). *Phys. Rev. A*, **6**, 1702-1709.
- Sternheimer, R. M. (1986). *Z. Naturforsch. Teil A*, **41**, 24-36.
- Stevens, E. D., DeLucia, M. L. & Coppens, P. (1980). *Inorg. Chem.* **19**, 813-820.
- Su, Z. (1993a). PhD thesis, State University of New York at Buffalo, USA.
- Su, Z. (1993b). *MOLPROP93, a Fortran Program for Calculating the Electrostatic Properties from the Multipole Description of the Charge Density*. Department of Chemistry, State University of New York at Buffalo, USA.
- Su, Z. & Coppens, P. (1992). *Acta Cryst.* **A48**, 188-197.
- Su, Z. & Coppens, P. (1994). *J. Appl. Cryst.* **27**, 89-91.
- Tsirel'son, V. G., Strel'tsov, V. A., Makarov, E. F. & Ozerov, R. P. (1987). *Sov. Phys. JETP*, **65**, 1065-1069.